Magnetic resonance investigation for a possible antiferromagnetic subphase in $(TMTTF)_2Br$

Mizue Asada[1] and Toshikazu Nakamura[1,2,*]

[1]*Institute for Molecular Science, Myodaiji, Okazaki 444-8585, Japan*

[2]*SOKENDAI (The Graduate University for Advanced Studies), Myodaiji, Okazaki 444-8585, Japan*

(Received 12 July 2017; revised manuscript received 6 August 2017; published 13 September 2017)

To understand the electronic states on the boundary region between the commensurate antiferromagnetic (II) phase and the incommensurate spin-density-wave phase in the generalized phase diagram for one-dimensional organic conductors, we performed antiferromagnetic resonance (AFMR) and nuclear magnetic resonance (NMR) measurements for $(TMTTF)_2Br$. The angular dependence of the AFMR fields at 1.5 K is different from that at 4.8 K, and the temperature dependence of the two AFMR modes is enhanced below 5 K. Furthermore, ^{2}D(Deuterium)-NMR measurements were performed for deuterated (TMTTF-d_{12})$_2$Br to investigate charge distribution by quadrupole splitting at low temperatures. We found that the ^{2}D-NMR spectrum changes at 4 K in the antiferromagnetic phase. Successive phase transition and a possible magnetic structure are discussed.

DOI: 10.1103/PhysRevB.96.125120

I. INTRODUCTION

One-dimensional (1D) conductors of the form $(TMTCF)_2X$ (C = S, Se) are some of the most extensively studied materials among organic conductors. They possess various ground states including the spin singlet (SS), commensurate antiferromagnetic (C-AF), incommensurate spin density wave (IC-SDW), and superconductivity (SC), with applied pressures or counter anions, denoted as X [1,2]. Here, commensurate refers to the case in which the AF wavelength matches the lattice constant. Moreover, findings of charge ordering (CO) and related phenomena in $(TMTTF)_2X$ have recently attracted significant attention [3,4]. According to recent developments for the TMTCF system [5–8], the generalized phase diagram is shown in Fig. 1. However, the origin of complex generalized phase diagrams remains unresolved. $(TMTTF)_2Br$ undergoes an antiferromagnetic transition at 16 K (T_N) [9]. Thus far, numerous studies have established that the ground state of $(TMTTF)_2Br$ is the C-AF (II) phase in the generalized phase diagram. However, it exists in the immediate vicinity of the IC-SDW phase.

Previously, the commensurate antiferromagnetic state of $(TMTTF)_2Br$ was confirmed by ^{13}C nuclear magnetic resonance (NMR) measurements [10,11]. At approximately the same time, we examined the magnetic structure of the antiferromagnetic state of $(TMTTF)_2Br$ by ^{1}H-NMR spectroscopy at 4.2 K [12]. The wave number of the antiferromagnetic state, $Q = (1/2, 1/4, 0)$, is commensurate with an amplitude of $0.14\,\mu_B$/molecule at 4.2 K. After that, the antiferromagnetic wave number of $(TMTTF)_2Br$ was also confirmed by ^{13}C-NMR measurements [13]. The spin arrangement was found to be -up-0-down-0- along the 1D molecular stacking direction (a axis). Recently, an anomalous change in the ^{13}C-NMR spectrum was also found below 4.2 K in the antiferromagnetic state of $(TMTTF)_2Br$ [14]. This observation suggests a possible change of electronic structure around 4.2 K. In the case of the ^{13}C nucleus, the large hyperfine coupling causes the NMR spectra to be extremely broadened in the antiferromagnetic state. Consequently, it is difficult to estimate subtle changes of electronic states. Hence, we investigated the antiferromagnetic resonance (AFMR) and ^{2}D-NMR measurements of a single crystal of $(TMTTF)_2Br$.

II. EXPERIMENT

The synthesis of pristine TMTTF and deuterated TMTTF-d_{12} molecules has been described in previous reports [15]. Deuterated TMTTF-d_{12} molecules, in which the protons ^{1}H of the end methylene group CH_3 are replaced by ^{2}D, are prepared by organic synthesis. Rectangular crystals of $(TMTTF)_2Br$ were prepared by an electrochemical oxidation of TMTTF in an acetonitrile (CH_3CN) solution under a constant current of 1.0 μA.

X-band electron spin resonance (ESR) experiments for a single crystal were conducted using Bruker Elexsys 500 with Oxford Cryostat E910. The temperature range was between 1.5 and 10 K. The single crystal was set in a quartz rod using silicone grease. The sample was placed such that a static magnetic field was applied to the $b'c^*$ plane. A precession goniometer stage was used for angle rotation measurements. The temperature variation of the ESR spectra was examined along the b' and c^* axes.

^{2}D-NMR measurements were performed on a deuterated (TMTTF-d_{12})$_2$Br single crystal in which ^{2}D nuclei are located on the end methylene group CD_3. A static magnetic field was applied in the $b'c^*$ plane and was fixed. But the exact angle cannot be determined since a coil was wound along the a axis. Pulsed-NMR measurements were performed at 55.001 MHz with typical pulse widths ($\pi/2$) of approximately 1.7 μs. The ^{2}D-NMR spectra were obtained by Fourier transformation of the spin-echo signals between 4 and 300 K. The spin-lattice relaxation rate T_1^{-1} was measured via magnetization recovery by integrating the intensities, including all lines of the Fourier-transformed spectra. The relaxation curve consisted of two components originating from two inequivalent CD_3 sites. Below the charge-ordering temperature T_{CO} (see below), the ^{2}D-NMR spectra became complicated. Hence, we estimated the spin-lattice relaxation rate from the initial curve, indicating the weighted average of all sites.

*t-nk@ims.ac.jp

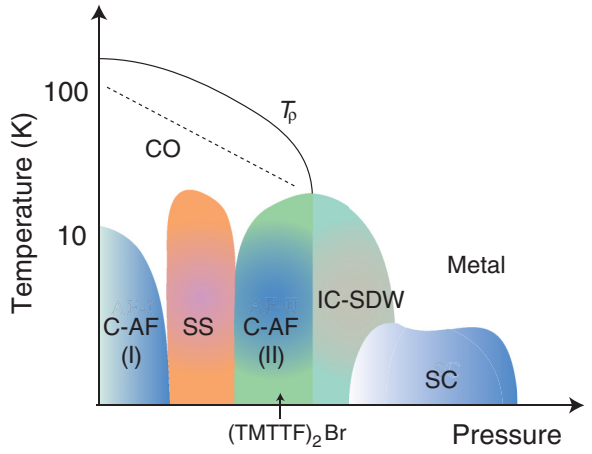

FIG. 1. Generalized phase diagram for (TMT*C*F)$_2X$ salts. C-AF (I) is the commensurate antiferromagnetic state at the low-pressure side, SS is the spin-singlet state, C-AF (II) is the commensurate antiferromagnetic state at the high-pressure side, IC-SDW is the incommensurate spin density wave, and SC is the superconducting state. CO is the charge-ordering phase observed at the intermediate-temperature region. T_ρ is the resistivity minimum temperature.

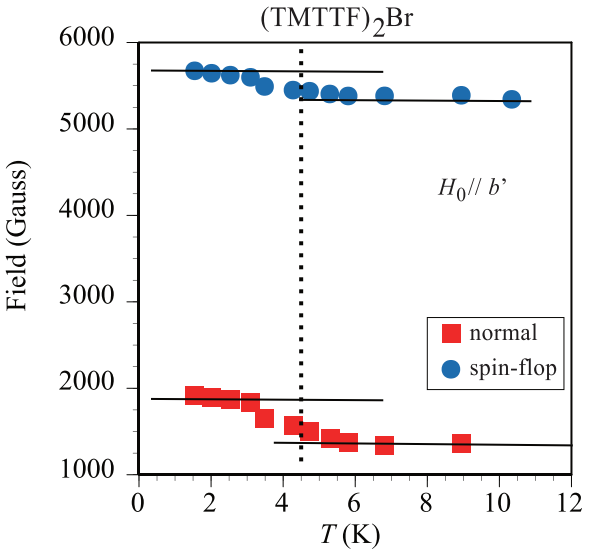

FIG. 3. Temperature dependence of the two antiferromagnetic resonance (AFMR) modes of (TMTTF)$_2$Br. The resonance at the lower field is the normal mode (square) and that at the higher field is the spin-flop mode (circle).

III. RESULTS AND DISCUSSION

For (TMTTF)$_2$Br salt, the antiferromagnetic structure is well explained by a two-sublattice model with three-axis anisotropy (orthorhombic) according to the previous AFMR measurements at 4.5 K by Parkin *et al.* [16]. It was also clarified that the antiferromagnetic easy, intermediate, and difficult axes are the b', c^*, and a axes, respectively. We also investigated the angular dependence of AFMR modes (normal mode and spin-flop mode) at 4.8 and 1.5 K, as shown in Fig. 2. The result at 4.8 K coincides with that of Parkin *et al.* at 4.5 K.

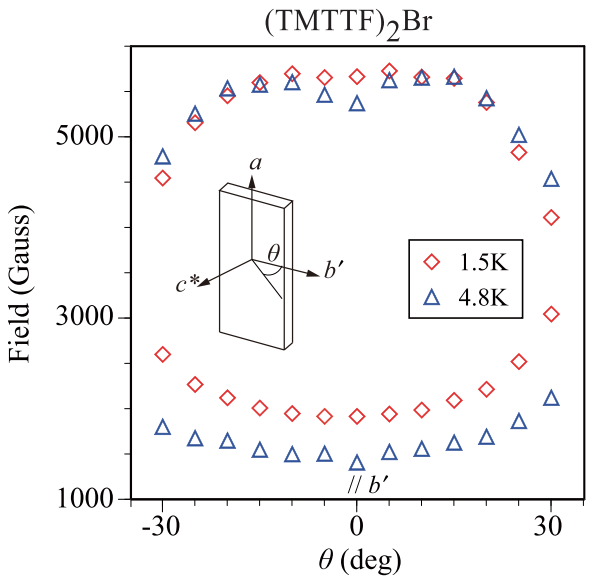

FIG. 2. Angular dependence of the two antiferromagnetic resonances (AFMR) of (TMTTF)$_2$Br at 4.8 K (triangle) and 1.5 K (diamond). The resonance at lower field is the normal mode and that of the higher field is the spin-flop mode.

Since stagger magnetization is developed in antiferromagnetic states and shows saturation just below T_N, the AFMR field is temperature independent at low temperatures in general. However, both AFMR fields of (TMTTF)$_2$Br at 1.5 K are enhanced compared to those at 4.8 K. The enhancement is more pronounced for the low-field normal mode.

The temperature dependence of the two AFMR modes was measured down to 1.5 K, as shown in Fig. 3. It shows an anomalous increase around 4 K. As mentioned above, the AFMR fields are temperature independent, in general, in the low-temperature region $T \ll T_N$. Moreover, the anomalous jump suggests a magnetic phase transition around 4 K.

Since the temperature dependence of the AFMR fields shows an anomaly, we consider it from the viewpoint of the fundamentals of AFMR. In a previous study [17], the antiferromagnetic resonance modes were calculated for a three-axial (orthorhombic) anisotropic antiferromagnet with two sublattices. According to the detailed analysis for the above sublattice antiferromagnetic system, a schematic field-frequency diagram of the calculated result of Ref. [17] (for the static field H_0 parallel to the easy axis) is shown in Fig. 4(a). The horizontal axis represents the magnetic field and the vertical axis represents the frequency. The two solid lines indicate the two AFMR modes. The lower resonance field is the normal mode and the higher one is the spin-flop mode. The dotted line going up to the right is the electron paramagnetic resonance (EPR) mode in which the resonance frequency is proportional to the external applied magnetic field ($g \sim 2$). When the external applied magnetic field (H_0) is less than the spin-flop field (H_{SF}), the resonance frequency of the normal mode decreases as H_0 increases, while that of the spin-flop mode increases as H_0 increases. At $H_0 = H_{SF}$, the resonance field of the normal mode reaches zero and then increase above H_{SF}. In contrast, the spin-flop mode jumps at $H_0 = H_{SF}$ and is constant above H_{SF}. Although the gap

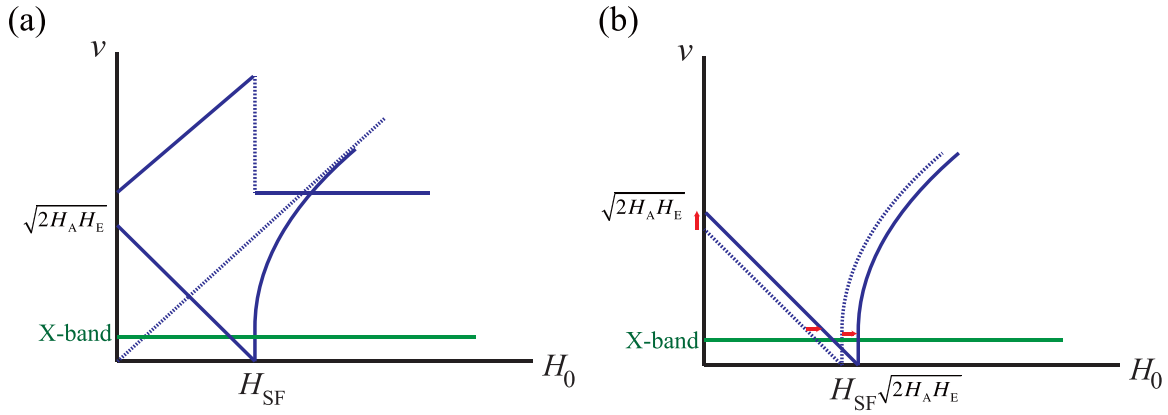

FIG. 4. (a) Schematic field-frequency diagram of the calculated results of AFMR for a three-axis (orthorhombic) anisotropic antiferromagnet with two sublattices. The resonance at the lower field is the normal mode and that at the higher field is the spin-flop mode. (b) Possible explanation for the shift of the AFMR fields. For the sake of clarity, only the spin-flop mode is shown.

(anisotropic energy) of the organic conductor $(TMTTF)_2Br$ is rather small, the microwave energy of the X band (0.3 K) is smaller than that of the gap. The relationship between the antiferromagnetic mode and microwave energy is also schematically shown in Fig. 4(a). Here, the spin gap is small but much higher than the microwave energy of the X band (0.3 K). The energy level of the X-band microwave is a horizontal line at the lower part of the figure. The AFMR magnetic fields in X-band measurements are the intersections of the solid lines. Below 4 K, the AFMR fields of both modes increase. Considering the schematic field-frequency diagram of AFMR from the calculated result, the enhancement of the AFMR field for both modes originates from the increases of the spin-flop field, H_{SF}, as shown in Fig. 4(b). Since the AFMR magnetic fields in X-band measurements are the intersections of the solid lines, they increase if H_{SF} increases. It is well known that $H_{SF} = \sqrt{2H_A H_E}$, where H_A is the anisotropic field and H_E is the exchange field [17,18]. In the case of $(TMTTF)_2Br$ salt, which is an organic radical $S = 1/2$ system, the anisotropic field H_A originates from the electronic magnetic dipole on other sites. However, such a large structural change seems unlikely to influence the H_A at an extremely low temperature of 4 K. The anisotropic field is not sensitive to electronic properties. Hence, it is natural to consider that the anomaly at 4 K originates from H_E. The exchange field H_E is proportional to the staggered magnetization of the sublattice M ($H_A = \lambda M$). Hence, it seems likely to be the origin of the AFMR field shift, if we suppose the increase of the staggered magnetization at 4 K. It should be noted that the staggered magnetization of the sublattice M is not always coincident with the amplitude of the antiferromagnet. A detailed discussion is presented later.

In order to clarify the electronic structure in the antiferromagnetic state from the microscopic point of view, we also performed ^{2}D-NMR measurements for deuterated $(TMTTF\text{-}d_{12})_2Br$. We choose deuterium ^{2}D nuclei for the following reasons. Since ^{1}H has a high gyromagnetic ratio, the broad NMR spectra in the antiferromagnetic state makes pulsed-NMR measurement difficult. ^{13}C has an excessively high hyperfine constant to obtain precise NMR spectra by the pulse method. Figure 5 shows the temperature dependence of the spin-lattice relaxation rate ^{2}D T_1^{-1} of $(TMTTF\text{-}d_{12})_2Br$. In the high-temperature region, the relaxation curve is composed of two components. Hence, we plot both the short and long components individually. TMTTF molecules stack to form a zigzag chain along the a axis. Hence, the methyl group is roughly divided into two sites, namely inner and outer sites. At low temperatures, ^{2}D T_1^{-1} is very long and the relaxation curve apparently seems to have a single component within the experimental error. Therefore, we tentatively plot the relaxation curve as a single component. Below 4 K, ^{2}D T_1^{-1} is too long to obtain precise NMR results. Note that $(TMTTF)_2Br$ undergoes the charge-ordering transition around 35 K (T_{CO}) [19] and antiferromagnetic transition at 16 K (T_N). (However, it is found that deuteration of TMTTF molecules enhances the charge-ordering transition temperatures for TMTTF family

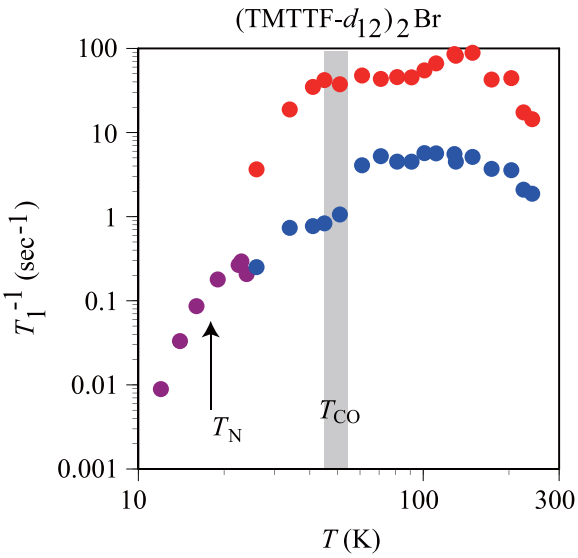

FIG. 5. Temperature dependence of the ^{2}D-NMR spin-lattice relaxation rate for deuterated $(TMTTF\text{-}d_{12})_2Br$ operated at 55.001 MHz. The charge-ordering transition temperature of $(TMTTF\text{-}d_{12})_2Br$ has not been estimated, but roughly estimated from that of $(TMTTF)_2Br$ considering Refs. [19,20] (hatched area).

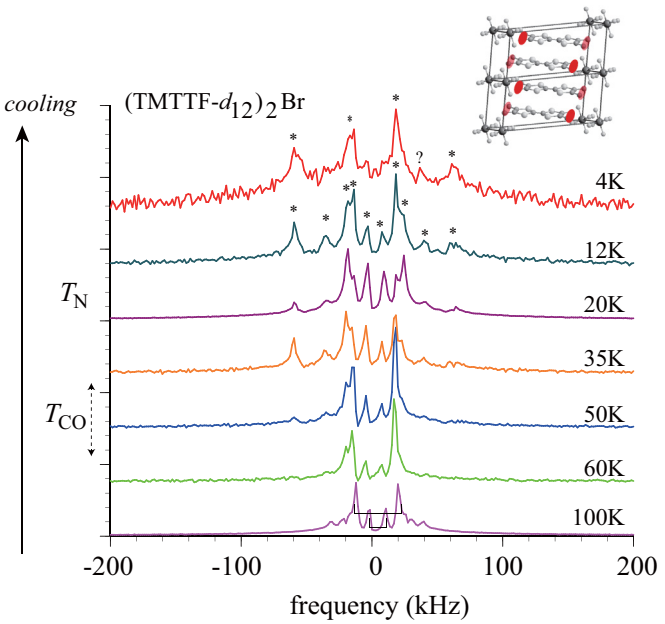

FIG. 6. Temperature dependence of the ^{2}D-NMR spectra for deuterated (TMTTF-d_{12})$_2$Br operated at 55.001 MHz. Each spectrum is composed of several doublets because of quadrupole splitting. Asterisks are added to compare spectra of 4 and 12 K.

salts about 20 K [20]. Hence we add roughly estimated charge-ordering transition temperature as the hatch in Fig. 5. The transition temperature of the ground state is not sensitive to deuteration.) In the high-temperature region ($T > T_{CO}$), the ^{2}D-NMR spin-lattice relaxation rate ^{2}D T_1^{-1} value was above 10 s^{-1} for the rapid component and above 1 s^{-1} for the slow component. Below T_{CO}, the ^{2}D T_1^{-1} rapidly decreases as the temperature decreases. It is also noted that the ^{2}D T_1^{-1} shows no enhancement (anomaly) around T_N. These observations indicate that the ^{2}D nuclear spin relaxation is not sensitive to the paramagnetic electron spins and that the ^{2}D nuclear quadrupole relaxation is dominant through the electric-field gradient due to the paramagnetic electron spins. As shown in Fig. 5, ^{2}D T_1^{-1} has a weak temperature dependence from room temperature down to T_{CO}. Since the (TMTTF)$_2X$ family salts are basically 1/4-filled systems, the electric charge fluctuates between TMTTF dimers. However, the electric charge freedom (charge fluctuation) is frozen below T_{CO}. Hence, the rapid decrease of ^{2}D T_1^{-1} can be well explained, assuming the locking of the electric-field gradient. The absence of any anomaly around T_N also supports the above inference. According to the ^{2}D T_1^{-1} results, the ^{2}D-NMR spectra reflect the charge state more than the spin state.

Figure 6 shows the temperature dependence of the ^{2}D-NMR spectra for deuterated (TMTTF-d_{12})$_2$Br operated at 55.001 MHz. It is found that the NMR spectra are composed of several doublets because of quadrupole splitting. The quadrupole splitting is proportional to the electric-field gradient. In the high-temperature region ($T > T_{CO}$), there are two doublets originating from two inequivalent sites. This observation is consistent with the observation of two components in the relaxation curve. Below T_{CO}, the ^{2}D-NMR spectra became complicated and broadened. The spectra are composed of several doublets, implying the symmetry breakdown of the charge configuration (increase of inequivalent CD_3 sites). It is reasonable that the TMTTF molecules are no longer equivalent below T_{CO}, and the charge-rich and charge-poor sites possibly cause a large field gradient. Both ^{2}D T_1^{-1} and the ^{2}D-NMR spectra are sensitive to the charge-ordering phase transition. On the other hand, at T_N, there is no significant change in the spectra as observed in ^{2}D T_1^{-1}. The ^{2}D-NMR is not sensitive to the magnetic interaction as observed in ^{2}D T_1^{-1}. However, it should be noted that the peak number decreases and a broad background appears at 4 K, suggesting that the charge (spin) configuration changes to incommensurate or inhomogeneous. In the case of the 1D IC-SDW state, the NMR spectra show powder-pattern-like spectra in which both ends of the absorption line diverge, and the structure inside disappears. Consequently, the number of absorption lines decreases. Moreover, note that AFMR fields show an anomalous enhancement around 4 K.

Previous NMR investigations for (TMTTF)$_2$Br showed that the antiferromagnetic state is commensurate with a wave number of (1/2, 1/4, 0), which were performed at 4.2 K [12,13]. Since the AFMR result indicates the enhancement of magnetization of the sublattice below 4 K, it seems likely that the antiferromagnetic magnetic structure changes at low temperatures. To understand the electronic state of the 1D system, the commensurability of the antiferromagnetic wave number is important. Note that the "incommensurate" SDW (IC-SDW) phase exists near the "commensurate" AF [C-AF (II)] phase of (TMTTF)$_2$Br. A schematic antiferromagnetic spin configuration for the 1/4-filled 1D system along the 1D chain is shown in Fig. 7. Figure 7(a) shows the spin configuration assuming the antiferromagnetic amplitude follows $A\sin(2k_F + \phi)$ with $\phi = 0$. The magnetic structure of (TMTTF)$_2$Br at 4.2 K is thought to have this configuration. The spin configuration of the molecules is repeated as -up-0-down-0- in this chain. This inference is consistent with the charge configuration in the charge-ordering state, which is -O-o-O-o- (o: charge-poor sites; O: charge-rich sites) along the a axis. This spin (charge) configuration is stable for off-site (long-range) Coulomb interaction, for which V is strong. On the next chain, the initial phase ϕ of the antiferromagnetic amplitude wave is shifted for the wave number (1/2, 1/4, 0). However, we can find the spin configuration of the repetition -0-down-0-up- in the next chain. Likewise, in the third chain, we can observe the spin configuration of the repetition -down-0-up-0-. Consequently, it is found that the average staggered magnetization of the sublattice $|\boldsymbol{M}_{AV}|$ is 0.5 at every chain, if we assume that the amplitude of the antiferromagnetic wave is normalized to 1.

The spin configuration assuming $A\sin(2k_F + \phi)$ with $\phi = \pi/4$ is shown in Fig. 7(b). In this case, the spin is repeated as -up-up-down-down- along the chains. This configuration is stable for conventional antiferromagnets and is advantageous to receive the benefit of the exchange interaction. The electronic charge is equivalent for all molecular sites, where the on-site (short-range) Coulomb interaction U is strong. If the screening effect becomes stronger through the itinerary characteristic of electrons, this magnetic structure is energetically more beneficial. In this case, the electron spin is -up-up-down-down-, and $|\boldsymbol{M}_{AV}|$ is 0.707 at every chain, assuming the amplitude of the antiferromagnetic wave is 1.

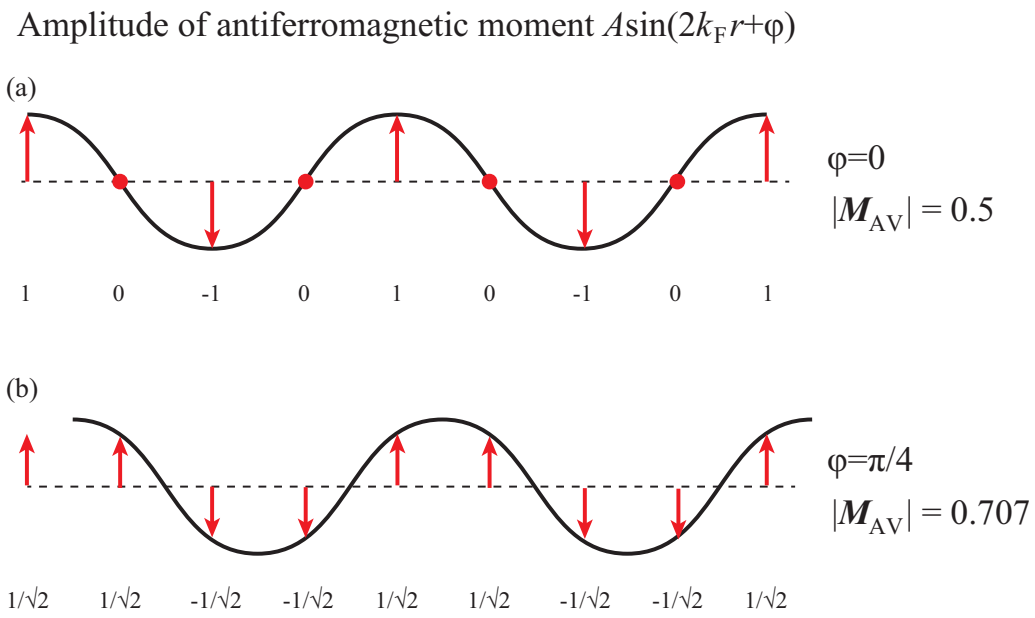

FIG. 7. Schematic antiferromagnetic spin configuration for 1/4-filled 1D system along the 1D chain. (a) Spin configuration assuming the antiferromagnetic amplitude follows $A\sin(2k_F + \phi)$ with $\phi = 0$. The magnetic structure of $(TMTTF)_2Br$ at 4.2 K is thought to have this configuration. (b) Spin configuration assuming $A\sin(2k_F + \phi)$ with $\phi = \pi/4$.

The above two cases are typical example of commensurate antiferromagnet for 1/4-filled systems. In the case of incommensurate wave number, the antiferromagnetic wavelength and lattice constant are not matching. The spin configuration on the molecules is no longer repeated in the different chains (periodicity changes when chain changes). As a result, the phase ϕ continuously changes as the chain changes.

Now, we discuss possible explanations for the anomaly at 4 K. As mentioned above, according to the previous NMR analyses, the magnetic structure along the 1D chain of $(TMTTF)_2Br$ is as shown in Fig. 7(a) [12,13]. What will happen if the phase of the AF wave changes while maintaining the amplitude? Let us consider the extreme case in which the phase ϕ changes from (a) 0 to (b) $\pi/4$. In this case, $|\boldsymbol{M}_{AV}|$ becomes 1.41 times that of the initial state. In the case of the ambient phases, $|\boldsymbol{M}_{AV}|$ is between (a) 0 and (b) $\pi/4$. Hence, $|\boldsymbol{M}_{AV}|$ always increases from the initial state if the phase ϕ changes, which can explain the anomalous enhancement of the AFMR field around 4 K. Based on this scenario, there are several causes for the *phase* changes. The first possibility is the simple spin-configuration change from -up-0-down-0- to -up-up-down-down-. The next possibility is the change from commensurate to incommensurate with decreasing temperature. Considering the AFMR and ^{2}D-NMR experimental results, the possibility of a simple phase change from -up-0-down-0- to -up-up-down-down- can be ruled out because, in this case, ^{2}D-NMR spectra should remain as multiple lines. On the other hand, a possible IC-SDW subphase transition at 4 K in $(TMTTF)_2Br$ can explain all the experimental results. Moreover, $(TMTTF)_2Br$ is located near IC-SDW in the generalized P-T phase diagram, as mentioned above. Considering that organic conductors show a large thermal contraction, it seems likely that the high-pressure phase becomes stable as the temperature decreases.

The last possibility is the discommensuration state in which the spin configuration is partially deformed. To our knowledge, there is no information on the order of the phase transition between C-AF (II) and IC-SDW. However, there is a possibility that a metastable discommensuration state (coexistence of inhomogeneous domains with antiferromagnetic states of different wave numbers) has occurred at the phase boundary. Actually, it has been pointed out that the C-AF (II) of $(TMTTF)_2Br$ is not simple: Anomalous behaviors were also reported even for C-AF (II) states of $(TMTTF)_2Br$ [21–23]. According to the literature [22], the ground state of $(TMTTF)_2Br$ under an application of a sufficient magnetic field is different from the conventional ground state. These authors claim the magnetic-field-induced density-wave (DW) glass state. Similar findings, i.e., glass transition and/or subphase in the spin-density-wave phase, have been discussed in the selenium substituted derivative $(TMTSF)_2X$ ($X = PF_6$, AsF_6, and ClO_4) [24–27]. The above models are basically based on a theoretical description of the strong pinning centers model in Refs. [21,28]. However, recently, a relaxation-time spectrum and the equilibrium heat capacity measurements have been performed for $(TMTTF)_2Br$ [29]. The thermal relaxation-time distribution function has a broad shape with low barrier height. According to the analysis result, the possibility of a tunneling process such as the strong pinning centers (soliton-antisoliton pairs) model is ruled out. There are a number of metastable states due to local deformations of the antiferromagnetic state. And the physical parameters are sensitive to the external magnetic field. According to the ^{2}D-NMR spectra, the peak number decreases and a broad background appears at 4 K, suggesting that the charge (spin) configuration changes to inhomogeneous or incommensurate, although microscopic magnetic structures cannot be identified. At present, the possibility of the discommensuration state cannot be ruled out.

IV. CONCLUSION

The ground state of $(TMTTF)_2X$ has been believed so far to be the C-AF (II) phase in the generalized phase diagram. Actually, the electronic state of $(TMTTF)_2Br$ at 4.2 K is clarified as a commensurate antiferromagnetic state with wave vector $Q = (1/2,1/4,0)$, and the spin configuration is -up-0-down-0-. We performed AFMR and ^{2}D-NMR measurement to understand the ground state of $(TMTTF)_2Br$. AFMR measurements show the increase of the staggered magnetization of the sublattice below 4 K. As for ^{2}D-NMR, the nuclear quadrupole relaxation was dominant through the electric-field gradient. According to the ^{2}D-NMR spectra, the peak number decreases and broad background appears at 4 K, suggesting that the charge (spin) configuration changes to inhomogeneous or incommensurate. Considering the AFMR and ^{2}D-NMR experimental results, the possible explanation of 4 K anomaly observed in $(TMTTF)_2Br$ is a commensurate to incommensurate successive phase transition. Although the steplike 4 K anomaly observed in AFMR supports a homogeneous phase transition, we cannot rule out the possibility of a homogeneous effect such as the discommensuration state at present. At least we can say that a phase ϕ change anomaly of antiferromagnetic spin configuration occurs around 4 K. It is also very surprising and intriguing that the submagnetic phase detected in the present work appears at a temperature around $T_N/4$. Similarly, $(TMTSF)_2X$ salts undergo subphases at $T_{SDW}/3$ in which there is a coexistence between charge density wave (CDW) and spin density wave (SDW) [26]. Further investigation is ongoing and supports from theoretical approaches for spin and charge distribution are awaited.

ACKNOWLEDGMENTS

The authors thank Professor Ohta (Kobe University) for a valuable discussion about AFMR, and Dr. Ihara and Professor Kawamoto (Hokkaido University) for a valuable discussion about NMR. This study was supported by a Grant-in-Aid for Scientific Research (B) (KAKENHI Grant No. 25287091) from JSPS.

[1] T. Ishiguro, K. Yamaji, and G. Saito, *Organic Superconductors*, 2nd ed. (Springer-Verlag, Berlin, 1998), and references therein.
[2] D. Jérome, Science **252**, 1509 (1991).
[3] D. S. Chow, F. Zamborszky, B. Alavi, D. J. Tantillo, A. Baur, C. A. Merlic, and S. E. Brown, Phys. Rev. Lett. **85**, 1698 (2000).
[4] P. Monceau, F. Y. Nad, and S. Brazovskii, Phys. Rev. Lett. **86**, 4080 (2001).
[5] B. Salameh, S. Yasin, M. Dumm, G. Untereiner, L. Montgomery, and M. Dressel, Phys. Rev. B **83**, 205126 (2011).
[6] F. Iwase, K. Sugiura, K. Furukawa, and T. Nakamura, Phys. Rev. B **84**, 115140 (2011).
[7] A. Pustogow, T. Peterseim, S. Kolatschek, L. Engel, and M. Dressel, Phys. Rev. B **94**, 195125 (2016).
[8] R. Świetlik, B. Barszcz, A. Pustogow, and M. Dressel, Phys. Rev. B **95**, 085205 (2017).
[9] P. Delhaes, C. Coulon, J. Amiell, S. Flandrois, E. Toreilles, J. M. Fabre, and L. Giral, Mol. Cryst. Liq. Cryst. **50**, 43 (1979).
[10] E. Barthel, G. Quirion, P. Wzietek, D. Jérome, J. B. Christensen, M. Jørgensen, and K. Bechgaard, Europhys. Lett. **21**, 87 (1993).
[11] B. J. Klemme, S. E. Brown, P. Wzietek, G. Kriza, P. Batail, D. Jerome, and J. M. Fabre, Phys. Rev. Lett. **75**, 2408 (1995).
[12] T. Nakamura, T. Nobutoki, Y. Kobayashi, T. Takahashi, and G. Saito, Synth. Met. **70**, 1293 (1995).
[13] S. Hirose, Y. Liu, and A. Kawamoto, Phys. Rev. B **88**, 125121 (2013).
[14] T. Isome, Y. Ihara, and A. Kawamoto (unpublished).
[15] K. Furukawa, T. Hara, and T. Nakamura, J. Phys. Soc. Jpn. **74**, 3288 (2005), and references therein.
[16] S. S. P. Parkin, J. C. Scott, J. B. Torrance, and E. M. Engler, Phys. Rev. B **26**, 6319(R) (1982).
[17] H. Ohta, N. Yamauchi, T. Nanba, M. Motokawa, S. Kawamata, and K. Okuda, J. Phys. Soc. Jpn. **62**, 785 (1993).
[18] M. Date, J. Phys. Soc. Jpn. **16**, 1337 (1961).
[19] T. Nakamura, J. Phys. Soc. Jpn. **72**, 213 (2003).
[20] F. Nad, P. Monceau, T. Nakamura, and K. Furukawa, J. Phys.: Condens. Matter **17**, L399 (2005).
[21] Y. N. Ovchinnikov, K. Biljaković, J. C. Lasjaunias, and P. Monceau, Europhys. Lett. **34**, 645 (1996).
[22] R. Melin, J. C. Lasjaunias, S. Sahling, G. Remenyi, and K. Biljaković, Phys. Rev. Lett. **97**, 227203 (2006).
[23] S. Sahling, J. C. Lasjaunias, R. Melin, P. Monceau, and G. Remeyi, Eur. Phys. J. B **59**, 9 (2007).
[24] J. C. Lasjaunias, K. Biljaković, F. Nad', P. Monceau, and K. Bechgaard, Phys. Rev. Lett. **72**, 1283 (1994).
[25] S. Valfells, P. Kuhns, A. Kleinhammes, J. S. Brooks, W. Moulton, S. Takasaki, J. Yamada, and H. Anzai, Phys. Rev. B **56**, 2585 (1997).
[26] K. Nomura, Y. Hosokawa, H. Iwasaki, S. Takasaki, J. Yamada, S. Nakatsuji, and H. Anzai, Synth. Met. **103**, 2147 (1999).
[27] M. Basletić, B. Korin-Hamzic, and K. Maki, Phys. Rev. B **65**, 235117 (2002).
[28] A. I. Larkin, Zh. Eksp. Teor. Fiz. **105**, 1793 (1994) [Sov. Phys. JETP **78**, 971 (1994)].
[29] S. Sahling, G. Remenyi, J. E. Lorenzo, P. Monceau, V. L. Katkov, and V. A. Osipov, Phys. Rev. B **94**, 144107 (2016).